

State-of-Polarization Monitoring Employing Optical Supervisory Channel Enabling Instantaneous Fluctuation Detection and Localization

Yusuke Sasaki, Masaki Sato, Hidemi Noguchi, and Kohei Hosokawa

Advanced Network Research Laboratories, NEC Corporation, 1753, Shimonumabe, Kawasaki, Kanagawa, 211-8666, Japan
yusuke-sasaki@nec.com

Abstract: We demonstrate a state of polarization monitoring system employing an optical supervisory channel can detect even short fluctuations of 10 μ s with precise localization in the experiment over an FPGA. © 2024 The Author(s)

1. Introduction

Optical network traffic increase has led to wide usage of the digital coherent transmission technology with digital signal processing (DSP). The network capacity in one single-mode fiber (SMF) can be twice by employing polarization division multiplexing (PDM) technology. A multiple-input multiple-output (MIMO) equalizer at the receiver side is used for compensation for the inter-polarization crosstalk and separation of signals because signals in each polarization are mixed through the PDM transmission. However, MIMO tracking error may occur when the state of polarization (SOP) change is abrupt and steep of larger than 50 kHz in the transmission line. This error may lead to signal-quality degradation and penalties of transmission systems [1]. It is essential to constantly monitor SOP changes to detect any failure of the optical transmission link and repair it to maintain transmission performance. The SOP change monitoring also enables the detection of a fiber break due to the shaking by digging near the fiber. The SOP change is generally caused by many reasons, for example, fiber squeezing, mechanical vibration, temperature fluctuation, lightning, and earthquakes. Several solutions have been proposed for SOP monitoring. Utilizing finite impulse response filter coefficients of MIMO equalizer enables to derive the SOP in the Stokes coordinates [2]. Requiring no extra measurement hardware, such as a polarimeter, is attractive. However, there is a limitation in monitoring speed due to the polarization-tracking performance of the MIMO equalizer since it uses the equalized signal. Fast SOP transients may also cause a loss of signal, making calculating the polarization rotation rate impossible. An SOP monitor using an optical supervisory channel (OSC) with polarization beam splitters and two photodiodes has been proposed [3]. This method enables span localization with a simple architecture. However, in this report, the frequency estimation needed to be more accurate, and the experiment was only performed on the continuous wave light. It is also needs to be clarified at what position where the SOP variation occurred within one span. Recently, we have demonstrated that this method is applicable to modulated light and in the existence of long-distance optical fibers in the transmission path and that the SOP change frequency can be estimated when the SOP fluctuations are in a steady state [4].

In this paper, we demonstrate the SOP-monitoring method employing the OSC with modulation can measure 10 μ s transients with the precise location identification. Both offline procedures using obtained data in the oscilloscope and FPGA indicate that the precise localization has been achieved with a 1% accuracy.

2. Concept and principle

The OSC is used in commercial optical transponder systems with the wavelength division multiplexing (WDM) to monitor and maintain the transmission lines and remotely control EDFAs. This OSC also carries information about the main signal such as wavelength channel number and condition of EDFA sites. On-off-keying modulation with an OC-3 156 Mb/s signal at 1510 nm is typically used for an OSC [5]. The OSCs are inserted into each EDFA node. The single-wavelength OSC optical signal outside the C-band is removed and added to the optical in-line EDFA system with couplers or filters. Adding SOP monitoring capability to the OSC enables localization of the span where the SOP changes because of the optical-span isolation of the OSC. When the SOP change occurs, the stokes parameter also changes. The Stokes parameter has four elements: S_0 , S_1 , S_2 , and S_3 . The S_0 reflects the total intensity of the light traveling a fiber. The S_1 reflects the linear polarization state of the light. The S_1 is depicted as $S_1 = 2I_0 - S_0$, where the I_0 is the intensity of the 0° polarized light wave, which can be measured with a polarizer [7]. When the optical power traveling the fiber is constant, the S_0 will also be constant. Measuring and monitoring I_0 enables S_1 variation detection, which leads to SOP monitoring.

3. Instantaneous fluctuation monitoring with localization

The OSC is inserted in each EDFA span; therefore, span localization is possible, but precise localization is complicated. By utilizing bi-directional transmission, precise localization will be possible. Fig. 1(a) shows a scheme of bi-directional transmission. The TX and RX are placed respectively on the east side and west sides, and the time clock signal is transmitted with main signals. The span distance is S . We assume SOP change occurs at a distance of X from the east side RX ($S-X$ from the west side RX). The t_0 is the time when the SOP change occurs. The east side RX receives SOP changed light at the time of t_1 , which is the time later than t_0 by the time necessary to propagate X . Similarly, the west side RX receives SOP changed light at the time of t_2 , which is the time later than t_0 by the time necessary to propagate $S-X$. Then, X is depicted as

$$X = \frac{S}{2} - \frac{c'}{2}(t_2 - t_1)$$

where c' is the transmission speed of the light in a fiber.

An ultra-fast SOP rotation up to 5.1 Mrad/s can be caused by lightning, and the SOP fluctuation continues only less than 100 μs [6]. The detection of 10 μs -length high-speed fluctuation is beneficial. The precise estimation of the SOP change location helps in the identification of SOP change causes. To demonstrate the scheme's effectiveness in Fig. 1(a), we conducted an experiment without bi-directional transmission. Fig. 1(b) shows the modified measurement setup. The operating wavelength of the laser diode (LD) was 1510 nm, and a modulator with 156 MHz on-off no-return-zero (NRZ) imitating the OC-3 was implemented [8]. A polarization scrambler was used as a SOP change source. The scrambler had electro-magnetic type six-quarter wave plates (QWPs) and a half-wave plate (HWP), which can be rotated at various speeds. The rotation of the wave plates causes SOP change, and the HWP-rotation speed (ν) determines the SOP change speed [9]. Instead of t_2 , we used the trigger signal from the scrambler synchronizing with SOP fluctuation as t_0 , which is the time when the SOP changes. Then, X can be derived from $X = c'(t_1 - t_0)$. The I_0 was transformed to the current value I_0' by the photodetector, and the I_0' was analyzed with filters to detect t_1 . This filter consisted of a high-pass filter to cut off the DC component and a low-pass filter to suppress the white noise, and the filters were designed to pass signals between 50 kHz and 500 kHz, which was our target SOP monitoring frequency range. The filter order of the high-pass filter was set to 201 taps, and the transition band was set to 20 kHz – 50 kHz. The low-pass filter was designed with 41 taps, and the transition band was designed as 500 kHz–600kHz. We set the SOP change duration time to 10 μs with an interval of 400 μs . The ν in this experiment was set from 50 kHz to 500 kHz, and the speeds of QWPs were set to sufficiently slower than HWP for randomizing SOP conditions. Fig. 1(c) shows signals obtained in the oscilloscope before filtering when the scrambler was located right after the modulator ($X = 50$ km) and right before the polarizer ($X = 0$ km), respectively. Fig. 1 (d) shows the ones after filtering. The noise was suppressed by filters and peaks due to SOP change can be seen clearly. The $t_1 - t_0$ was derived by peak searching of the filter-treated signal of I_0' as Fig. 1(d). We derived X , and Fig. 1 (e) and (f) show the histograms of the estimated X when the scrambler was located at 25 km ($X = 25$ km) and 50 km ($X = 50$ km) with various ν , respectively. The estimated distances were 25.3 km and 50.4 km, which well matched with the fiber spans. This result indicates that the filter setting worked well.

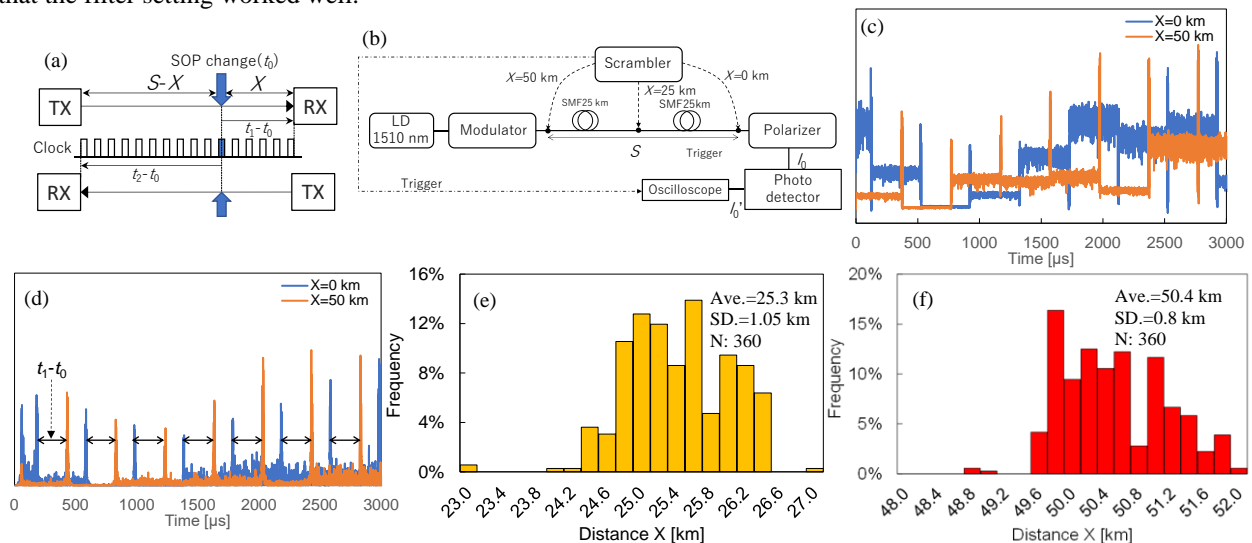


Fig. 1. (a) Scheme of SOP localization, (b) Measurement setup for localization, (c) Obtained data before filtering, (d) Data after filtering (e) Estimated distance distribution when X is 25 km and (f) 50 km.

4. FPGA implementation

We applied the previous measurement scheme to the FPGA, assuming practical usage. The measurement setup employing an FPGA (AMD ZCU111) is shown in Fig. 2(a). A 1562 nm 10 Gbps SFP+ transmitter was used to generate the clock signal with a 64-bit length. The TX and RX were always synchronized. After 50-km fiber transmission, the 1562 nm signal and the OSC signal at 1510 nm were separated by a WDM filter. The OSC signal was converted to the electrical signals via a photodetector with a bandwidth of 5 GHz, and then was digitalized in the ADC and processed in the FPGA. The clock signal was recovered from the 1562 nm signal received by the SFP+. Fig. 2(b) describes the signal processing procedure in the FPGA. Because the minimum sampling rate of the ADC installed in the ZCU111 was limited to 1 GHz, and because it was difficult to design a steep filter that passed between 50 kHz and 500 kHz, we first performed down-sampling consisting of 1/32 and 1/16 from 1105.92 MHz to 2.16 MHz. Since the ADC of the FPGA had a sampling speed limitation of 1 Gbps, and it was not easy to design a filter that did not cause the anti-aliasing, an electrical filter of 10.7 MHz was inserted before the ADC. The signals after down-sampling were filtered whose setting was the same as the previous section. Since the bit rate of the ADC was 12 bits, we designed the filter coefficients and the internal calculations as 24 bits so that the effect of bit rounding was minimized. Fig. 2 (c) shows an example of the obtained data when we set the ν as 100 kHz and the scrambling duration time as 10 μ s. The time interval between each trigger edge and peak corresponds to the time to propagate from the location of the scrambler to the receiver ($X = 0$). Fig. 2 (d) and (e) show the histogram of the estimated distance when the scrambler was located at the receiver side and after the coupler ($X = 50$ km). The estimated distance at $X = 0$ was 13 km, not 0 km. It was owing to the signal processing delay inside the FPGA and the time gap between the trigger and scrambling of the scrambler. The average value difference was 49.7 km, which matched well with the fiber span of 50 km. It is confirmed that the proposed system can identify where the SOP fluctuation has occurred.

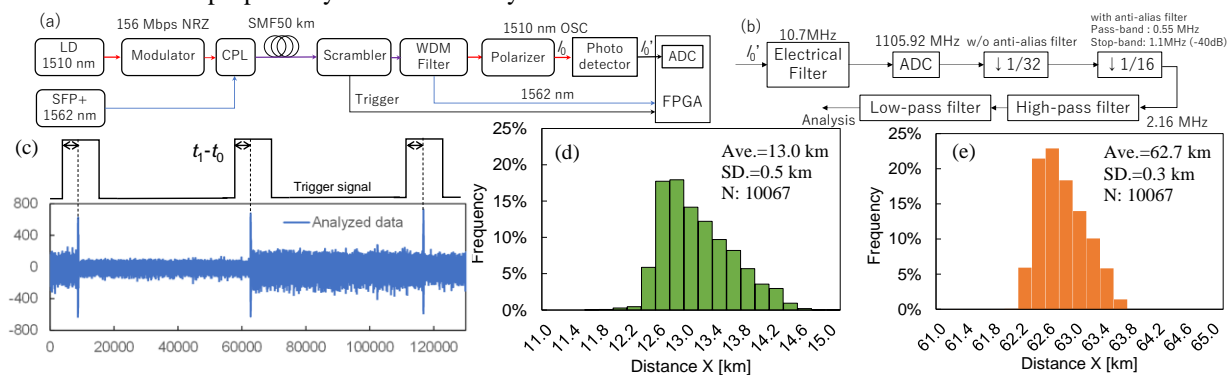


Fig. 2. (a) Measurement setup employing an FPGA, (b) Processing procedure in FPGA, (c) Data after filtering and trigger pulse, (d) Estimated distance from the receiver side when the scrambler was located at the receiver side and (f) after the coupler.

5. Conclusion

We demonstrated that an optical supervisory channel can be used as the monitor of instantaneous SOP fluctuation with precise position localization. This method is beneficial to adding SOP monitoring function to optical transmission lines because this method does not require expensive measurement instruments.

Acknowledgment

These research results were obtained from the commissioned research (No.0470102) by National Institute of Information and Communications Technology (NICT), Japan.

6. References

- [1] P. M. Krummrich et al., "Demanding response time requirements on coherent receivers due to fast polarization rotations caused by lightning events", *Opt.Express*, vol. 24, no.11, pp. 12442-12457 (2016)
- [2] T. Ye et al., "A polarization change monitor by eigenvalue analysis in coherent receiver", *OFC2019*, M4I.1.
- [3] J. E. Simsarian and P. J. Winzer, "Shake Before Break: Per-Span Fiber Sensing with In-Line Polarization Monitoring," *OFC2017*, M2E.6.
- [4] Y. Sasaki et al., "State-of-Polarization Monitoring Employing Optical Supervisory Channel with Modulated Light," *2023 Opto-Electronics and Communications Conference (OECC)*, Shanghai, China, 2023, pp. 1-3, doi: 10.1109/OECC56963.2023.10209582.
- [5] C. Sarker, "Optical Supervisory Channel Implementation," *International Journal of Scientific & Engineering Research*, vol. 3, Issue 11, pp. 1-3 (2012)
- [6] D. Charlton et al., "Field measurements of SOP transients in OPGW, with time and location correlation to lightning strikes", *OpticsExpress*, vol. 25, no.9, pp.9689-9696 (2017)
- [7] R. Perkins and V. Gruev, "Noise modeling of Stokes parameters in division of focal plane polarization imagers," *2011 IEEE International Symposium of Circuits and Systems (ISCAS)*, Rio de Janeiro, Brazil, 2011, pp. 1828-1831, doi: 10.1109/ISCAS.2011.5937941.
- [8] Telcordia GR-253-CORE issue4, December 2005
- [9] R. Noe and B. Koch, "Emulation of polarization fluctuations in glass fibers caused by lightning strikes," *Photonic Networks; 19th ITG-Symposium*, pp. 1-4 (2018)